

OPTIMAL PUMP FREQUENCY FOR AC HYSTERETIC SQUID

Andrey L. Pankratov*

Institute for Physics of Microstructures of RAS, Nizhny Novgorod, RUSSIA.

This paper presents the analytical and numerical analysis of fluctuational dynamics of ac hysteretic SQUID. It has been demonstrated, that the most important parameter for the improvement of the hysteretic SQUID sensitivity is the ratio between the pump and the characteristic frequencies but not their absolute values. The resonant behavior of signal-to-noise ratio as function of the pump frequency has been observed and the narrow area for the optimal pump frequency range is indicated.

It is well known [1],[2],[3] that the slope of a signal characteristic of hysteretic ac SQUID $h = dV_{ac}/d\Phi$ increases with increasing the working (pump) frequency and therefore output energy sensitivity becomes considerably better. Noise properties of ac SQUIDS were intensively investigated both for cases $\Omega \ll 1$ and $\Omega \gg 1$ (where $\Omega = \omega/\omega_c$, ω is the pump frequency and ω_c is the characteristic frequency of Josephson junction (JJ)) [4],[5],[6]. It has been demonstrated that increasing of frequency without violation of working capacity of SQUID is possible nearly up to the characteristic frequency of JJ [7], which may be of the order of 1 THz for JJ based on low T_c materials and 10 THz - for high T_c ones. Besides, it was reported [8] about ac SQUID with $\Omega = 0.1$, demonstrated high sensitivity about $4 \cdot 10^{-32}$ J/Hz. So, elaboration and fabrication of a single junction SQUID working in microwave frequency range looks very promising, and usual opinion is that increasing of the pump frequency may allow to reach, in principle, such high characteristics as dc SQUIDS have.

However, at the present time, there is still no at least qualitative understanding at which pump frequency a microwave SQUID should operate to reach the maximal sensitivity, since due to mathematical problems no investigations were performed in the most interesting pump frequency range $\omega \sim \omega_c$. As follows from recent results by Cheska [9], there should not be such optimal pump frequency for a nonhysteretic SQUID, which is not surprising since that is a (quasi) linear system. The ac hysteretic SQUID, is, however, strongly nonlinear system, and, recently, in qualitatively similar model system, the resonant behavior of signal-to-noise ratio as function of frequency of driving signal has been observed [10].

The present paper is devoted to studying the nonlinear fluctuational dynamics of a hysteretic ac SQUID in the pump frequency range around ω_c . The effect of suppression of noise by strong periodic signal [10] has for the first time been observed in the model, describing the real electronic device: it has been demonstrated that there exists a certain optimal pump frequency range at which the hysteretic SQUID will operate with minimal noise-

induced error and that there is an optimal driving amplitude at which the voltage-flux characteristic is the most close to the noiseless case.

Theory of a single junction SQUID is already quite well developed (see, e.g., [1]-[3] and references therein). Necessary requirements for SQUIDS operating in hysteretic mode are the following: $\ell \geq 1$ to provide hysteresis and maximize nonlinearity (where $\ell = L/L_0$, L is the inductance of the ring, $L_0 = \Phi_0/(2\pi I_c)$, I_c is the critical current of the JJ, Φ_0 is the flux quantum) and $\beta = 2\pi I_c R_N^2 C/\Phi_0 \ll 1$ (the SQUID should be overdamped) to prevent from stochasticity when switching between states with different trapped fluxes in the SQUID ring (here $R_N^{-1} = G_N$ is the normal conductivity of the JJ, C is the capacitance).

The fluctuational dynamics of a flux in a SQUID ring coupled to a resonator may be described by the following equations:

$$\dot{\varphi} + \ell \sin \varphi + \varphi - \varphi_m - \alpha_s \psi(t) = \varphi_F(t), \quad (1)$$

$$\frac{1}{\omega_0^2} \ddot{\psi} + \frac{\eta_r}{\omega_0} \dot{\psi} + \psi = \alpha_r (\varphi - \varphi_m) + a \sin(\omega_0 t). \quad (2)$$

Here $\varphi = \frac{2\pi\Phi}{\Phi_0}$, Φ is the trapped flux, $\varphi_m = \frac{2\pi\Phi_m}{\Phi_0}$, Φ_m is the measured flux and $\psi(t)$ is the pump signal from the resonator, time is normalized to the characteristic frequency of the SQUID $\omega_s = \omega_c/\ell = R_N/L$, $\omega_c = 2\pi R_N I_c/\Phi_0$ - characteristic frequency of JJ, η_r is the damping of the resonator, α_s and α_r are coupling coefficients of the SQUID ring and the resonator, respectively, and $\omega_0 = \omega_r/\omega_s$ is the dimensionless pump frequency.

Let us take into account only internal thermal fluctuations in the SQUID ring. In this case the noise source $\varphi_F(t)$ may be represented by the white Gaussian noise:

$$\langle \varphi_F(t) \rangle = 0, \quad \langle \varphi_F(t) \varphi_F(t + \tau) \rangle = 2\gamma \ell \delta(\tau), \quad (3)$$

where $\gamma = 2\pi k_B T/(\Phi_0 I_c)$ is the dimensionless noise intensity, T is the temperature and k_B is the Boltzmann constant.

Let us first consider analytically and numerically the fluctuational flux dynamics of a SQUID

ring, supposing that the signal from the resonator is known: $\alpha_s \psi(t) = A \sin(\omega_0 t + \xi)$, where A is the driving amplitude and ξ is the initial phase. In this case the required statistical characteristics may be computed on the basis of the transitional probability density $W(\varphi, t)$. It is well known, that the Fokker-Planck equation (FPE) for the probability density $W(\varphi, t)$ corresponds to Eq. (1) for the flux:

$$\begin{aligned} \frac{\partial W(\varphi, t)}{\partial t} &= -\frac{\partial G(\varphi, t)}{\partial \varphi} = \\ &= \frac{\partial}{\partial \varphi} \left\{ \left[\frac{du(\varphi, t)}{d\varphi} W(\varphi, t) \right] + \gamma \ell \frac{\partial W(\varphi, t)}{\partial \varphi} \right\}, \end{aligned} \quad (4)$$

where

$$u(\varphi) = -\ell \cos(\varphi) + (\varphi - \varphi_e)^2/2 \quad (5)$$

is the dimensionless potential profile, $\varphi_e = \varphi_m + A \sin(\omega_0 t + \xi)$ is the external flux. The initial and boundary conditions for Eq. (4) are as follows:

$$W(\varphi, 0) = \delta(\varphi - \varphi_0) \text{ and } G(\pm\infty, t) = 0.$$

The quantity, that reflects the noise induced transition process from the metastable state is a probability $P(t) = \int_{-\infty}^d W(\varphi, t) d\varphi$ that transition will not occur at the moment of time t , that we will call the survival probability, where d is some boundary point, usually a potential barrier top.

To describe analytically the survival probability one can recourse to the adiabatic approximation, that for the case of a weak periodic driving has been used in the context of stochastic resonance [11],[12]. It has been demonstrated in [13] (see also [14]) that for the case of a metastable potential and strong periodic driving the evolution of survival probability in the frequency range $0 \leq \omega_0 < 0.5$ may be well described by a modified adiabatic approximation, which allows to extend the usual analysis to arbitrary driving amplitudes and noise intensities. For simplicity, let us consider the case for $\varphi_m = \pi$ (bistable potential), then the survival probability may be written in the form:

$$\begin{aligned} P(\varphi_0, t) &= g(t) \left[P(\varphi_0, 0) + \int_0^t \frac{dt'}{g(t')\tau_q(\varphi_0, t')} \right], \quad (6) \\ g(t) &= \exp \left\{ - \int_0^t \left[\frac{1}{\tau_p(\varphi_0, t')} + \frac{1}{\tau_q(\varphi_0, t')} \right] dt' \right\}, \end{aligned}$$

where $\tau_p(\varphi_0, t')$ is the exact mean decay time of the left metastable state obtained for the corresponding time-constant potential [15],[14]:

$$\begin{aligned} \tau_p(\varphi_0) &= \frac{1}{\gamma \ell} \left\{ \int_{\varphi_0}^d e^{u(y)/\gamma \ell} \int_{-\infty}^y e^{-u(x)/\gamma \ell} dx dy + \right. \\ &\quad \left. + \int_d^c e^{u(y)/\gamma \ell} dy \int_{-\infty}^d e^{-u(x)/\gamma \ell} dx \right\}. \end{aligned} \quad (7)$$

Here $c > d$ is the coordinate of the right potential minimum at the moment when $\sin(\omega_0 t + \xi) = 1$ and the left minimum disappears. The time scale τ_q is the decay time of the right metastable state and is calculated from the same formula (7) where in the potential (5) the phase of the driving signal is changed from 0 to π . Note that with respect to the usual adiabatic analysis the approximate Kramers' time has been substituted by the exact one (7) and a surprisingly good agreement of this approximate expression with the computer simulation results has been found in rather broad range of parameters, that is seen in Fig. 1.

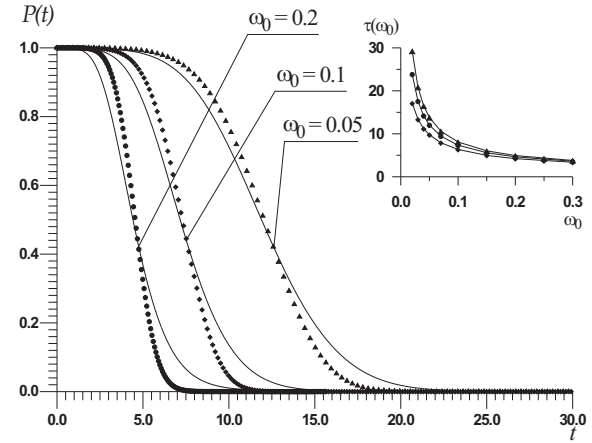


Fig. 1. The evolution of survival probability; dots - computer simulations, solid line - modified adiabatic approximation. Inset: the mean transition time; dots - computer simulations, solid line - modified adiabatic approximation; $\gamma = 0.04; 0.1; 0.2$ from top to bottom.

In Fig. 1 the probability evolution is presented for $\gamma = 0.1$, $A = 3$, $\xi = 0$ and $\varphi_m = \pi$. The adiabatic approximation is drawn by solid line, while the results of numerical solution of Eq. (4) by dots. One can see, that the coincidence is good enough. Even better agreement between the modified adiabatic approximation (6), (7) and the computer simulation results may be observed for the mean decay time of the left metastable state (inset of Fig. 1). Since the working conditions for the considered potential are such that during half of the driving period T_ω the survival probability monotonically changes from unity to almost zero, we can define the mean decay time in time-periodic potential as:

$$\tau_p(\omega_0) = \frac{\int_0^{T_\omega/2} [P(t) - P(0)] dt}{P(T_\omega/2) - P(0)}. \quad (8)$$

The definition (8) is analogous to widely used definition of integral relaxation time for diffusion in time-constant potentials (see [14] and references therein). As it is seen from the inset of Fig. 1, in the range of validity of adiabatic approximation the mean decay time (8) computed using formu-

las (6),(7) gives perfect coincidence with the results of computer simulation. It is intriguing to see that there is a range of driving frequencies $0.1 \leq \omega_0 \leq 0.3$, where the mean decay time is almost insensitive to the noise intensity: the curves for different noise intensities actually coincide that constitutes the effect of suppression of noise by a strong periodic signal. This effect may also be demonstrated by the analysis of the signal-to-noise ratio R . In accordance with [12] we denote R as:

$$R = \frac{1}{S_N(\omega_0)} \lim_{\Delta\omega \rightarrow 0} \int_{\omega_0 - \Delta\omega}^{\omega_0 + \Delta\omega} S(\omega) d\omega, \quad (9)$$

where $S(\omega) = \int_{-\infty}^{+\infty} e^{-i\omega\tau} K[\tau] d\tau$ is the spectral density, $S_N(\omega_0)$ is noisy pedestal at the driving frequency ω_0 and $K[\tau]$ is the correlation function: $K[\tau] = \langle\langle \varphi(t+\tau)\varphi(t) \rangle\rangle$, where the inner brackets denote the ensemble average and outer brackets indicate the average over initial phase ξ . In order to obtain $K[\tau]$ the Eq. (4) has been solved numerically for $A = 3$, $\ell = 3$, $\varphi_m = \pi$.

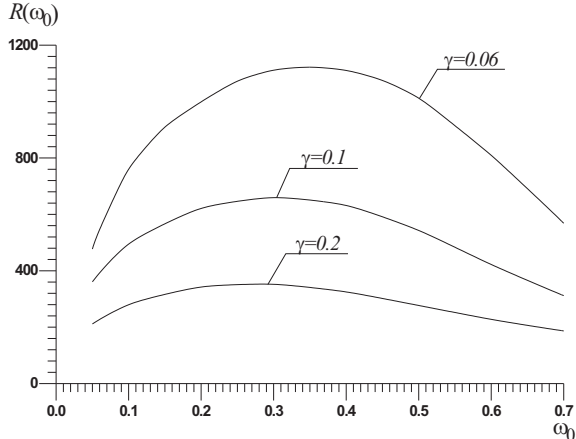


Fig. 2. The signal-to-noise ratio as function of driving frequency.

Let us plot the signal-to-noise ratio (SNR) as function of driving frequency ω_0 . From Fig. 2 one can see, that R as function of ω_0 has strongly pronounced maximum. The location of this maximum lies below the cut-off frequency ($\omega_0 = 1$ or $\omega_s = R_N/L$ in dimensional notations) and depends on the driving amplitude A and noise intensity. The existence of optimal driving frequency may be explained in the following way: with increase of frequency noise-induced escapes occur at lower barrier, and the maximum of SNR corresponds to the lowest barrier, that is closest to the dynamical case, where the transition occur when the barrier completely disappears. With further increase of frequency, there is not enough time for transition in the absence of noise and SNR drops, while the mean transition time rises [10],[13].

One can solve numerically the system of equations (1) and (2) and compute ac current-voltage characteristic and voltage-flux characteristic.

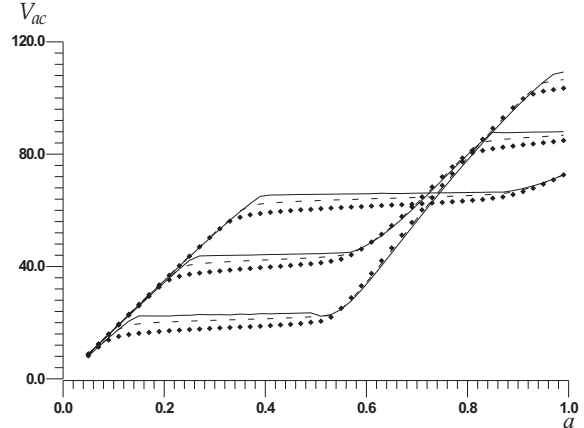


Fig. 3. The ac current-voltage characteristic for $\omega_0 = 0.01$; solid line - $\gamma = 0$, dashed line - $\gamma = 0.01$, diamonds - $\gamma = 0.03$.

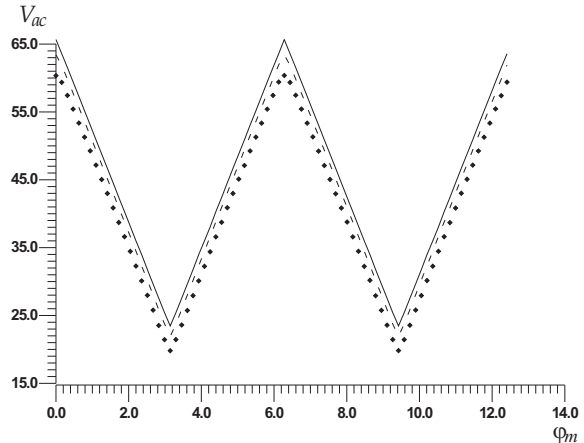


Fig. 4. The voltage-flux characteristic for $\omega_0 = 0.01$; solid line - $\gamma = 0$, dashed line - $\gamma = 0.01$, diamonds - $\gamma = 0.03$.

In Fig. 3 the ac current-voltage characteristic ($V_{ac}(a) = \sqrt{2\psi^2}$, $\varphi_m = 0; \pi/2; \pi$) is presented for $\omega_0 = 0.01$ that corresponds to relatively low frequency case and for the following parameters: $\ell = 3$, $\eta_r = 0.01$, $\alpha_s \alpha_r / \eta_r = 2$. As it is seen, for the case $\gamma = 0$ the plateaus are nearly horizontal. For $\gamma = 0.01$ and $\gamma = 0.03$ the plateaus have a tilt and lie below the curves for $\gamma = 0$. The voltage-flux characteristics for the same parameters and $a = 0.47$ is presented in Fig. 4. It is seen that with increase of noise intensity γ the corresponding curves move down and their edges are rounded. Low frequency interference, as well as noise of the resonator and amplifiers (that were not taken into account in the present paper) will make the situation only worse and the quantity of splitting of the curves for different γ will give the error of the measured flux φ_m . Fortunately, with the increase of

the pump frequency the picture changes radically: already at $\omega_0 = 0.1$ the plateaus for $\gamma = 0.01$ cross the plateaus for $\gamma = 0$ at certain points. With approaching the maximum of signal-to-noise ratio $\omega_0 \approx 0.3$ (Fig. 2) the crossing points move to the middle of the plateau and for different γ become more close to each other, see Fig. 5.

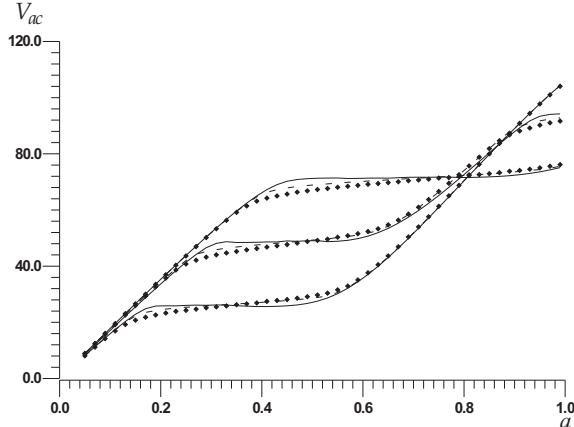


Fig. 5. The ac current-voltage characteristic for $\omega_0 = 0.3$; solid line - $\gamma = 0$, dashed line - $\gamma = 0.01$, diamonds - $\gamma = 0.03$.

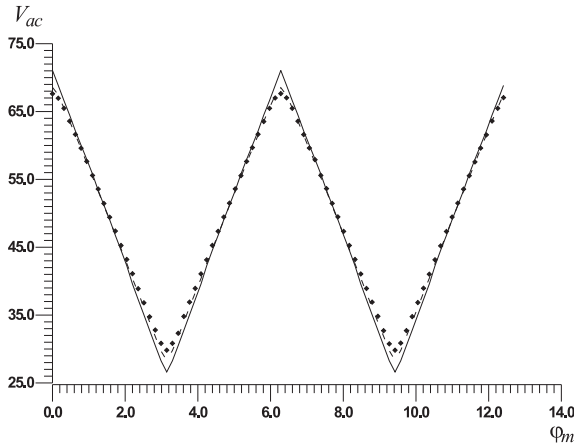


Fig. 6. The voltage-flux characteristic for $\omega_0 = 0.3$; solid line - $\gamma = 0$, dashed line - $\gamma = 0.01$, diamonds - $\gamma = 0.03$.

It is intuitively obvious that to reach the maximal sensitivity of the SQUID, the voltage-flux characteristic should be computed for the pump amplitude a , corresponding to the crossing point of plateaus for $\varphi_m = \pi/2$ (see analogous consideration for dc SQUIDS in [16]). In Fig. 6 the voltage-flux characteristic is plotted for $\omega_0 = 0.3$, $a = 0.51$ and $\gamma = 0; 0.01; 0.03$. It is seen, that there is a broad range of φ_m , $0.7 \leq \varphi_m \leq 2.2$, where curves for different γ coincide and, therefore, noise actually do not affect the SQUID in this range of parameters. If, however, the measured flux lie outside the range $0.7 \leq \varphi_m \leq 2.2$, some known quantity of magnetic flux φ_n may be added to shift the working point to this region, precise measurements may

be performed, and φ_n may be extracted to get information about the original measured flux.

Up to date tendency in ac SQUID development is increasing the pump frequency up to microwave range ($\sim 10GHz$) in order to reduce the noise [3] with respect to measured voltage and thereby to increase the sensitivity of devices of this kind. However, as follows from the above presented analysis, the main optimizational parameter of the microwave hysteretic SQUID is the ratio between the pump and the characteristic frequencies $\omega_0 = \omega_r \ell / \omega_c$, but not their absolute values; it must be in the range $\omega_0 \approx 0.2 - 0.4$ in order to get maximal sensitivity of the SQUID. Also during measurements, very important parameter is the amplitude of ac driving. It can be chosen from ac current-voltage characteristic of the SQUID as the point, where the plateau for $\Phi_m = \Phi_0/4$ for a given temperature $k_B T \neq 0$ crosses the plateau for $k_B T = 0$; the calibration can be done once by cooling the SQUID to a low temperature.

The author wishes to thank V. V. Kurin and Yu. N. Nozdrin for helpful discussions. The work has been supported by the Russian Foundation for Basic Research (projects 00-02-16528, 02-02-16775, 02-02-17517, 02-02-06126, and 00-15-96620) and by INTAS (projects 01-0367 and 01-0450).

* Electronic address: alp@ipm.sci-nnov.ru

- [1] K. K. Likharev, *Dynamics of Josephson junctions and circuits*, Gordon and Breach, 1986.
- [2] A. Barone and G. Paterno, *Physics and Applications of the Josephson Effect*, Wiley, 1982.
- [3] D. Koelle, R. Kleiner, F. Ludwig, E. Dantsker and J. Clarke, *Rev. Mod. Phys.* **71**, 631 (1999).
- [4] J. Kurkijarvi, *J. Appl. Phys.* **44**, 3729 (1973).
- [5] V. V. Danilov and K. K. Likharev, *Radiotekhnika i Elektronika*, No. 8, 1725 (1980) [*Radio Eng. and Electron. Phys.* 25, No. 8, 112 (1980)].
- [6] O. V. Snigirev, *Radiotekhnika i Elektronika*, No. 10, 2178 (1981) (in Russian).
- [7] R. A. Buhrman and L. D. Jackel, *IEEE Trans. Magn.* **13**, 879 (1977).
- [8] A. P. Long, T. D. Clark and R. J. Prance, *Rev. Sci. Instr.* **51**, 8 (1980).
- [9] B. Chesca, *J. Low Temp. Phys.* **110**, 963 (1998).
- [10] A. L. Pankratov, *Phys. Rev. E* **65**, 022101 (2002).
- [11] B. McNamara and K. Wiesenfeld, *Phys. Rev. A* **39**, 4854 (1989).
- [12] L. Gammaitoni, P. Hanggi, P. Jung and F. Marchesoni, *Rev. Mod. Phys.* **70**, 223 (1998).
- [13] A. L. Pankratov and M. Salerno, *Phys. Lett. A* **273**, 162 (2000).
- [14] A. N. Malakhov and A. L. Pankratov, *Adv. Chem. Phys.* **121**, 357 (2002).
- [15] A. N. Malakhov, *Chaos* **7**, 488 (1997).
- [16] G. V. Prokopenko et. al., *IEEE Trans. Appl. Supercond.* **11**, 1239 (2001).